Japanese Journal of
Applied Physics

The Japan Society of Applied Physics

REGULAR PAPER

Thermally induced evolution of on-surface-synthesized crown ether polymers on Cu(111): transition from semiconductor chains to metallic nanoflakes

To cite this article: Toyo Kazu Yamada *et al* 2026 *Jpn. J. Appl. Phys.* **65** 05SP24

View the article online for updates and enhancements.

You may also like

- Halogen derivatives of benzo- and dibenzocrown ethers: synthesis, structure, properties and application
S M Pluzhnik-Gladyr
- Crown Ethers in Nonaqueous Electrolytes for Lithium/Air Batteries
Wu Xu, Jie Xiao, Deyu Wang et al.
- On-surface synthesis on a bulk insulator surface
Antje Richter, Andrea Floris, Ralf Bechstein et al.

This content was downloaded from IP address 133.82.251.191 on 17/03/2026 at 07:13

Japanese Journal of Applied Physics **65**, 05SP24 (2026) **REGULAR PAPER**
https://doi.org/**10.35848/1347-4065/ae498f**

Thermally induced evolution of on-surface-synthesized crown ether polymers on Cu(111): transition from semiconductor chains to metallic nanoflakes

Toyo Kazu Yamada[1,2*], Tomoya Kashiwagi[1], and Masaki Horie[3]

[1]*Department of Materials Science, Chiba University, 1-33 Yayoi-Cho, Inage-Ku, Chiba 263-8522, Japan*
[2]*Molecular Chirality Research Centre, Chiba University, 1-33 Yayoi-cho, Inage-Ku, Chiba 263-8522, Japan*
[3]*Research Institute for Electronic Science, Hokkaido University, N21W10, Kita-Ward, Sapporo 001-0021, Japan*

[*]E-mail: toyoyamada@faculty.chiba-u.jp

Received January 14, 2026; revised February 19, 2026; accepted February 23, 2026; published online March 12, 2026

We present a scanning tunneling microscopy study of on-surface synthesis using bromine-terminated crown ether (BrCR) molecules adsorbed on Cu(111) under ultra-high vacuum. Although theoretical models predict that high-temperature annealing yields energetically stable linear or trident-linked crown ether (CR) structures forming ordered two-dimensional (2D) networks, our experiments reveal alternative reaction pathways. A self-assembled BrCR monolayer prepared at 300 K with semiconducting characteristics transforms into one-dimensional polymer chains upon annealing at 450–500 K. In contrast, annealing at 600–700 K induces a drastic transition to 2D nanoflakes with metallic properties. This transformation is accompanied by a significant reduction in apparent molecular height and pronounced changes in the local density of states. These results demonstrate that annealing temperature enables controlled tuning of CR-derived nanocompounds and electronic properties from semiconducting to metallic. © 2026 The Japan Society of Applied Physics. All rights, including for text and data mining, AI training, and similar technologies, are reserved.

1. Introduction

Crown ether (CR) molecules have been intensively studied over the past decades because their cyclic structure enables the encapsulation of guest species within the ring, forming host–guest complexes.[1–9] In particular, CR rings have been modelled as molecular "wheels" that can be combined with axially coordinated ferrocene-based guest molecules serving as "axles," enabling the realization of functional wheel-and-axle-type molecular machines. This concept has been successfully demonstrated in previous studies.[4,10] These results also represent a significant milestone in surface science, as they enabled the realization of ferrocene on noble metal surfaces at 300 K without molecular decomposition. Ferrocene is otherwise known to decompose upon direct contact with noble metal substrates.[11,12] The encapsulation by CRs provides both physical trapping and electronic decoupling from the metal substrate, thereby preserving the quantum spin properties of the guest molecule. While ferrocene has a singlet ground state ($S = 0$),[4] related metallocenes such as nickelocene, with a triplet ground state ($S = 1$), have been proposed as potential molecular quantum bit (qubit) candidates when protected by CR encapsulation. Another important functionality of CR molecules is their ability to trap transition metal atoms, leading to the formation of transition-metal nanoclusters with sizes of approximately 1.5 nm, which can be exploited as catalytic centers.[13]

CR molecules with these unique properties can be further functionalized by introducing terminal halogen atoms, enabling each molecule to serve as a precursor for intermolecular coupling and the formation of polymers via on-surface synthesis. In particular, Br_4-dibenzo crown ethers (BrCR) can undergo on-surface Ullmann coupling upon post-annealing at 400–500 K under ultra-high vacuum (UHV) conditions on a Cu(111) surface, resulting in one-dimensional (1D) polymer chains extending over several tens of nanometers.[5] However, several fundamental questions remain unresolved. Under these relatively low annealing temperatures, polymer growth proceeds through intermediate bonding configurations between BrCR precursors. Specifically, although each BrCR molecule carries two bromine atoms on one side of the ring, typically only one C–Br bond is cleaved and participates in intermolecular coupling, while the second bromine atom either remains intact or binds to substrate metal adatoms. As a consequence, the resulting polymers adopt a winding, nonlinear structure.[5] Interestingly, theoretical studies predict that these intermediate configurations are not energetically favorable.[5] Instead, bonding geometries with connection angles of 120° and 180°, corresponding to the trident and linear configurations, respectively, are expected to be the most stable and second most stable arrangements, as illustrated in Fig. 1(a).

In this study, we therefore investigate whether a two-dimensional (2D) self-assembled monolayer (SAM) of CR molecules, which is stable at 300 K, can be transformed into a 2D polymeric monolayer film by higher-temperature annealing in the range of 600–700 K. Moreover, we demonstrate a drastic change in the electronic nature of the CR-derived compounds, from semiconducting to metallic behavior. The surface morphology and electronic structures were studied by employing scanning tunneling microscopy and spectroscopy (STM/STS) at 300 K in UHV.

2. Experimental methods

2.1. UHV STM/STS measurements

STM measurements were carried out using a home-built UHV STM system consisting of separate STM, sample preparation, and deposition chambers. The base pressures of the STM, preparation, and deposition chambers were below 5.0×10^{-8} Pa, 2.0×10^{-8} Pa, and 1.0×10^{-7} Pa, respectively. Samples and STM tips were transferred between chambers via transfer rods without breaking UHV conditions, and the chambers were isolated by gate valves. Electrochemically etched tungsten tips were used for all STM measurements. Tip preparation was performed either by conventional chemical etching followed by thermal flashing up to 2000 K under UHV conditions[14]

© 2026 The Japan Society of Applied Physics. All rights, including for text and data mining, AI training, and similar technologies, are reserved.

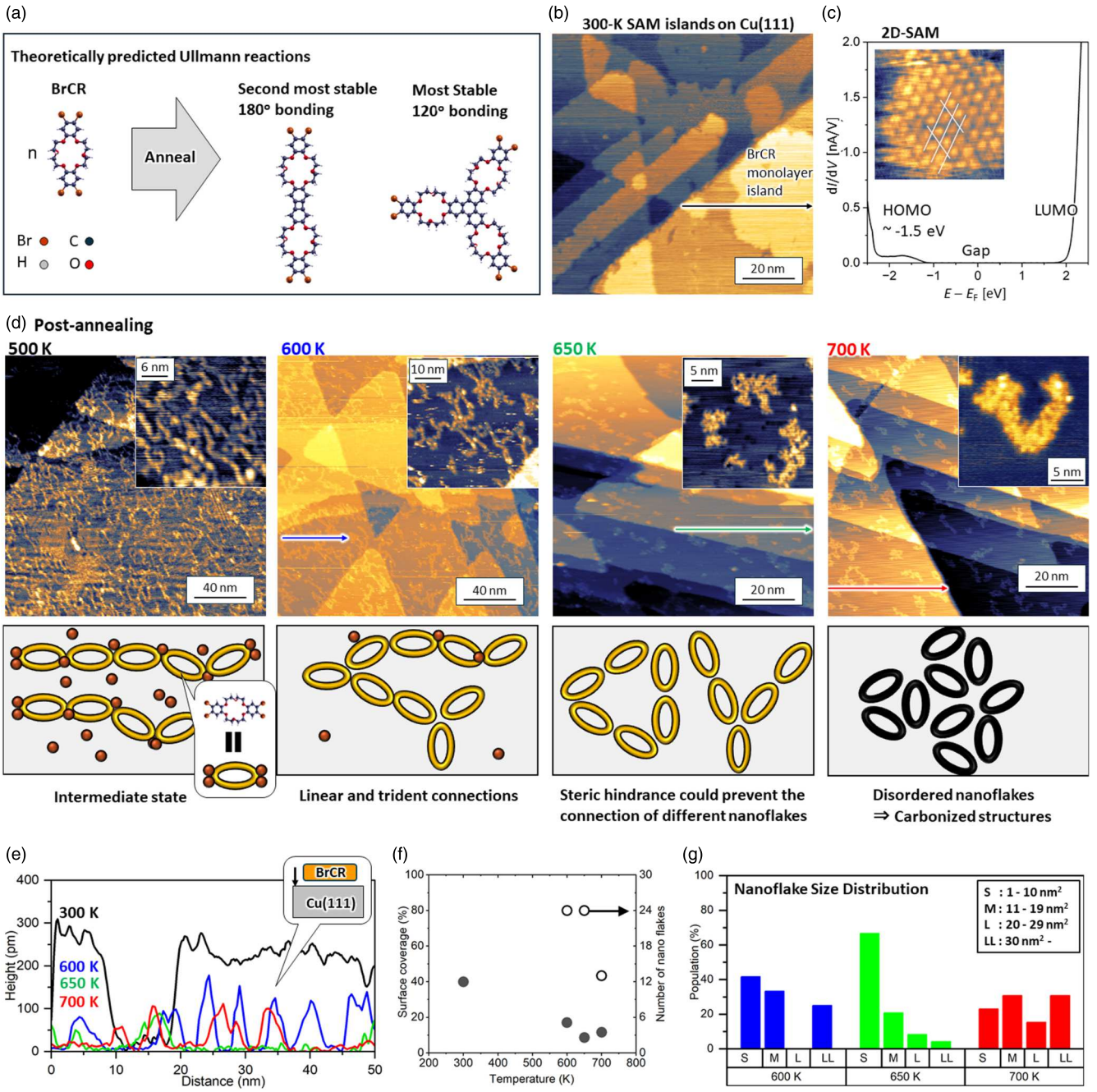

Fig. 1. Temperature-dependent evolution of BrCR monolayer films on Cu(111) upon thermal annealing. (a) Theoretically predicted BrCR-linked models corresponding to energetically stable configurations. (b) STM topographic image of a BrCR self-assembled monolayer (SAM) formed on Cu (111) at 300 K under UHV conditions (100 × 100 nm^2, $V_s = -2.5$ V, $I_t = 20$ pA). (c) *dI/dV* spectrum acquired on the BrCR SAM array. The inset shows a high-resolution STM topographic image of an ordered BrCR SAM (10 × 10 nm^2, $V_s = -2.5$ V, $I_t = 10$ pA). (d) Series of STM topographic images of 0.4 ML BrCR on Cu(111) after thermal annealing for 10 min in UHV at 500, 600, 650, and 700 K (from left to right). Image sizes and tunneling parameters are 200 × 200 nm^2 ($V_s = -2.5$ V, $I_t = 20$ pA), 200 × 200 nm^2 ($V_s = -1.5$ V, $I_t = 5$ pA), 100 × 100 nm^2 ($V_s = -2.5$ V, $I_t = 5$ pA), 100 × 100 nm^2 ($V_s = -2.5$ V, $I_t = 5$ pA), respectively. The insets show magnified views of the corresponding regions: 30 × 30 nm^2 ($V_s = -2.5$ V, $I_t = 20$ pA), 50 × 50 nm^2 ($V_s = -1.5$ V, $I_t = 5$ pA), 30 × 30 nm^2 ($V_s = -2.0$ V, $I_t = 5$ pA), 20 × 20 nm^2 ($V_s = -2.5$ V, $I_t = 20$ pA), from left to right. (e) Height profiles of BrCR SAM islands (black) and nanoflakes formed after annealing at 600 K (blue), 650 K (green), and 700 K (red) along the arrows in (b) and (d). (f) Surface coverage of nanoflakes as a function of annealing temperature. (g) Nanoflake size distribution after annealing at 600 K (blue), 650 K (green), and 700 K (red).

or by flame etching in air,[15,16] which produces sharp tips within approximately 3 s. Topographic STM images were acquired in constant-current mode using a Nanonis BP4 SPM controller. STS measurements were conducted to probe the local density of states (LDOS) of the sample surfaces. Tunneling current $I(V)$ spectra were recorded as a function of sample bias voltage, typically ranging from −2 V to +2 V, with the feedback loop disabled. The acquired $I(V)$ curves were numerically differentiated to obtain differential conductance (dI/dV) spectra, which are proportional to the product of the LDOS and the exponential tunneling background, $T = \exp(-2\kappa z)$, where κ is the decay constant and z is the tip–sample separation.[17,18] STM and STS data were analyzed using WSxM (version 5.0 Develop 10.2) and Gwyddion (version 2.53) software packages.[19]

© 2026 The Japan Society of Applied Physics. All rights, including for text and data mining, AI training, and similar technologies, are reserved.

2.2. Sample preparations

An atomically flat and clean Cu(111) surface was used as the substrate.[5,13] The Cu(111) crystal was mounted on a heating stage located at the center of the preparation chamber. Surface cleaning was performed by Ar^+ ion sputtering at a sample temperature of 300 K for 15 min, followed by annealing to 873 K for 15 min using electron bombardment heating. This sputtering–annealing cycle was repeated several times until a clean and well-ordered Cu (111) surface was obtained, typically exhibiting atomic terraces with widths of approximately 100 nm and a characteristic Cu surface-state peak at −0.4 eV below the Fermi energy.[20]

Br_4-dibenzo crown ethers: 4,4′,5,5′-tetrabromodibenzo [18]crown-6 ethers (BrCR) were placed in an alumina crucible and sublimated by gentle radiative heating using a tungsten filament in the deposition chamber. The crucible temperature was monitored with an alumel–chromel thermocouple. During molecular deposition, the Cu(111) substrate was positioned approximately 200 mm above the crucible. Prior to BrCR deposition, the deposition rate was calibrated using a quartz crystal microbalance (QCM).[21]

After deposition, the sample was transferred to a heating stage at the center of the preparation chamber, where a tungsten filament was positioned approximately 2 mm behind the sample. Radiative heating from the filament gently heated the molybdenum sample holder beneath the Cu(111) crystal, thereby indirectly heating the Cu substrate. Sample temperatures below 700 K were measured using a thermocouple, while temperatures above 700 K were monitored with an optical pyrometer (Japan Sensor Co., FTZ6-P300-10S22; emissivity $\varepsilon = 0.1$).

3. Results and discussion

3.1. BrCR Ullmann reaction on Cu(111) at 600–700 K

Figure 1(b) shows an STM topographic image of the pristine SAM islands of BrCR molecules on Cu(111), formed at 300 K under UHV conditions. In the STM image, brighter contrast indicates regions of higher apparent topographic height. The inset of Fig. 1(c) shows a magnified image of the interior of the island, revealing an array of bright spots. These spots reflect the molecular morphology combined with the spatial distribution of the molecular LDOS. The periodic lattice is indicated by white lines in the inset of Fig. 1(c), showing that a single unit cell measures approximately 1 nm × 2 nm at 300 K, including the effect of thermal drift. This value is comparable to the molecular unit dimensions of 0.90 nm × 1.74 nm previously reported from STM measurements performed at cryogenic temperatures (4 K and 78 K).[4–6]

Figure 1(c) presents representative differential conductance (dI/dV) spectra acquired on the BrCR SAM, with the inset displaying the periodic 2D molecular array. The spectra reveal distinct features corresponding to the highest occupied molecular orbital (HOMO) at approximately −1.5 eV and the lowest unoccupied molecular orbital at approximately +2.0 eV. A clear energy gap is observed around the Fermi level ($E - E_F = 0$), indicating semiconducting electronic behavior of the BrCR monolayer.

Figure 1(d) presents a series of large-area STM topographic images of approximately 0.4 monolayers (ML) of BrCR molecules on Cu(111), acquired at 300 K after thermal annealing at 500, 600, 650, and 700 K (from left to right). The left two panels cover areas of 200 × 200 nm^2, while the right two panels show 100 × 100 nm^2 images. In all cases, identical amounts of BrCR (corresponding to a nominal thickness of approximately 0.25 nm) were deposited at a rate of ∼0.1 nm min^{-1}, as monitored by a QCM. The insets show magnified images, and the lower panels present schematic models of CR ring molecules, illustrating how changes in their connections can lead to the formation of nanoflakes from 1D polymer chains.

After annealing at 500 K, the surface is predominantly covered with 1D polymer chains [left panel of Fig. 1(d)], consistent with a previous report.[5] A central objective of this study is to determine whether these intermediate 1D polymer structures can further evolve into the theoretically predicted final configurations shown in Fig. 1(a). To this end, the sample was annealed to higher temperatures.

Following annealing at 600 K, 1D polymer chains are still observed. In contrast to the surface after annealing at 500 K, the surrounding terraces are largely free of impurity patches, which were previously abundant. This suggests that the Br atoms cleaved during the Ullmann reaction either desorb from the surface, diffuse along step edges, or form Cu–Br bonds that contaminate the surface, thereby resulting in relatively flat terraces between the CR polymers. Nevertheless, the polymers largely retain their 1D character, indicating that the structures remain kinetically stable.

Upon further annealing to 650 K, a drastic change is observed in the STM topographic images [Fig. 1(d)]. The 1D polymer chains decrease, indicating that the intermediate states are no longer stable at this temperature. If BrCR polymerization proceeded exclusively via the Ullmann coupling pathways predicted in Fig. 1(a), the formation of extended, ordered 2D networks would be expected. Instead, molecular nanoflakes are formed, as highlighted in the enlarged STM images shown in the insets of Fig. 1(d). After annealing at 650 K, the nanoflakes appear to consist of assemblies of CR molecules.

The proposed model explains why nanoflakes form instead of extended 2D ordered networks. At 650 K on Cu(111), CR molecules undergo debromination, generating reactive carbon sites that preferentially bond with carbon atoms of neighboring CR molecules. However, once 1D chains have formed, long-range diffusion becomes unfavorable, as it would require breaking existing C–C bonds before reconnecting with other CR units. Instead, it is energetically more favorable for additional CR molecules to attach while preserving the original C–C bonds, thereby introducing branching points and converting linear connections into trident junctions. As a result, rather than forming long 1D chains, the polymers bend and assemble into triangular and Y-shaped structures, both exhibiting C_3 symmetry [see the model at 650 K in Fig. 1(d)]. Once nanoflakes with sizes of approximately 5–10 nm are formed, steric hindrance imposed by confinement to the 2D surface suppresses further interconnection between nanoflakes at 650 K, leading to the stabilization of mixed triangular- and Y-shaped nanoflakes on the surface.

Finally, upon annealing the sample to 700 K, further structural changes occur. At this temperature, only

© 2026 The Japan Society of Applied Physics. All rights, including for text and data mining, AI training, and similar technologies, are reserved.

nanoflakes are observed, and the 1 nm wide stripe features are no longer present [Fig. 1(d)].

A pronounced structural transformation is further evidenced by changes in the apparent molecular height following thermal annealing. As shown in Fig. 1(e), pristine BrCR molecules in the SAM exhibit an apparent height of approximately 230 pm relative to the Cu(111) surface. In contrast, annealing above 600 K results in a drastic reduction of the apparent height to approximately 100 pm. This substantial decrease indicates significantly stronger interactions between the molecular species and the Cu substrate. In Fig. 1(e), the black, blue, green, and red profiles correspond to the measurements taken before annealing (300 K) and after annealing at 600, 650, and 700 K, respectively, along the arrows indicated in Figs. 1(b) and 1(d).

Another notable observation is the substantial reduction in molecular coverage after annealing at temperatures between 600 and 700 K. Figure 1(f) quantifies the relative surface coverage of CR species as a function of annealing temperature, revealing a pronounced decrease at higher temperatures. Specifically, the surface coverage of CR-derived nanocompounds decreases to less than 50% of that of the BrCR SAM prior to annealing, as indicated by the black dots in Fig. 1(f): the coverage is reduced from 40% (0.4 ML) to approximately 20% (0.2 ML). This behavior suggests that, during the transition from intermediate to final states, fragments such as bromine atoms, Cu adatoms, and patch-like CR residues detach from the polymer chains and subsequently diffuse to step edges or desorb from the surface. In addition, the final bonding configurations likely favor denser packing of CR-derived species, as indicated by the number of nanoflakes [white circles in Fig. 1(f)]. Although the number of nanoflakes decreases by approximately half from 650 K to 700 K, the overall surface coverage remains nearly constant, leading to their aggregation into nanoflakes and a concomitant increase in the uncovered surface area.

Figure 1(g) further illustrates the evolution of the nanoflake size distribution with annealing temperature. The nanoflakes are classified by their areal size (nm^2) as *S*: 1–10 nm^2, *M*: 11–19 nm^2, *L*: 20–29 nm^2, and LL: $\geqslant$30 nm^2. The size distribution changes systematically with increasing annealing temperature. In particular, long chains that remain after annealing at 600 K, classified as LL, drastically decrease after annealing at 650 K and transform into nanoflakes; this drastic change is clearly reflected in Fig. 1(g). Following annealing at 700 K, smaller nanoflakes appear to aggregate, leading to the formation of larger nanoflakes.

3.2. Drastic electronic structure changes induced by thermal annealing

The pronounced transformation of CR-derived species into nanoflakes on Cu(111) was further examined using STS. Figure 2 shows simultaneously acquired STM and STS data for a 0.4 ML BrCR layer on Cu(111) measured at 300 K after successive thermal annealing at 600, 650, and 700 K. Rows (a)–(c) display STM topographic images, the corresponding d*I*/d*V* maps recorded over the same surface areas, and representative d*I*/d*V* spectra obtained from the CR-derived nanoflakes (red curves) and the surrounding terrace regions (black curves), respectively.

A direct comparison of the STM topographies in Fig. 2(a) with the corresponding d*I*/d*V* maps in Fig. 2(b) reveals that the molecular nanoflakes appear darker in the d*I*/d*V* maps, indicating a lower LDOS compared to the surrounding terrace regions. This contrast suggests that the terrace regions exhibit a more metallic electronic character. Notably, the characteristic LDOS peak at −0.4 eV associated with the surface state of clean Cu(111) is absent,[22,23] and the d*I*/d*V* signal near the Fermi level is close to 0.0 nA V^{-1}. These observations indicate that the terraces are atomically flat, as shown in Fig. 1(d). However, the d*I*/d*V* spectra suggest that the terraces do not correspond to a clean Cu (111) surface and were likely contaminated during the annealing process. This implies that the Cu surface is either covered by or chemically bonded to bromine atoms released from the BrCR molecules during the Ullmann coupling reaction.

An important observation is that the nanoflakes formed after annealing at 600 and 650 K still exhibit discernible HOMO features [red arrows in Fig. 2(c)]. These features are distinct from the LDOS spectra of the surrounding terrace regions, indicating that the nanoflakes and terraces possess different electronic structures. A remarkable feature observed in Fig. 2(c) is that the CR-derived nanoflakes exhibit an extremely narrow, nearly vanishing electronic gap. Specifically, the d*I*/d*V* signal does not drop to zero, in sharp contrast to the BrCR SAM shown in Fig. 1(c), which displays a clear band gap exceeding 2 eV. This result indicates that thermal annealing at 600–650 K induces a transition in the electronic properties of CR from semiconducting to metal-like behavior.

These nanoflakes undergo further electronic changes after annealing at 700 K [Fig. 2(c)]. At this temperature, their d*I*/d*V* spectra become indistinguishable from those of the surrounding terrace regions and show neither distinct peaks nor shoulder-like LDOS features in the vicinity of the Fermi energy, indicating the absence of well-defined molecular orbitals. Together with the STM topographic observations shown in Fig. 1(d), these results indicate that annealing at 700 K promotes surface coating by species originating from CR decomposition. This interpretation is consistent with previous reports showing that C–H bonds can transform into C=C covalent bonds at temperatures above 650 K, as observed during the on-surface synthesis of graphene nanoribbons from molecular precursors.[24] Moreover, the CR ring itself may undergo substantial structural rearrangement into entirely different configurations. Similar thermally induced structural transformations have been reported for related systems on Au and Ag surfaces.[7] Thus after the 700 K annealing the CR-derived nanoflakes could be changed to carbonized structures.

The height profiles shown in Fig. 1(e), together with the electronic structure measurements in Fig. 2, suggest that the CR-derived nanoflakes are located closer to the Cu substrate. Before annealing at 300 K, BrCR exhibits semiconducting behavior, whereas after annealing at 600–700 K, the resulting nanoflakes display metallic characteristics. For a semiconducting molecule with lower conductivity than the surrounding Cu substrate, the STM tip may record a lower apparent height due to the reduced tunneling current. In contrast, if the CR-derived nanoflakes are metallic and have conductivity comparable to that of the Cu substrate, the apparent height would be expected to increase, provided that

© 2026 The Japan Society of Applied Physics. All rights, including for text and data mining, AI training, and similar technologies, are reserved.

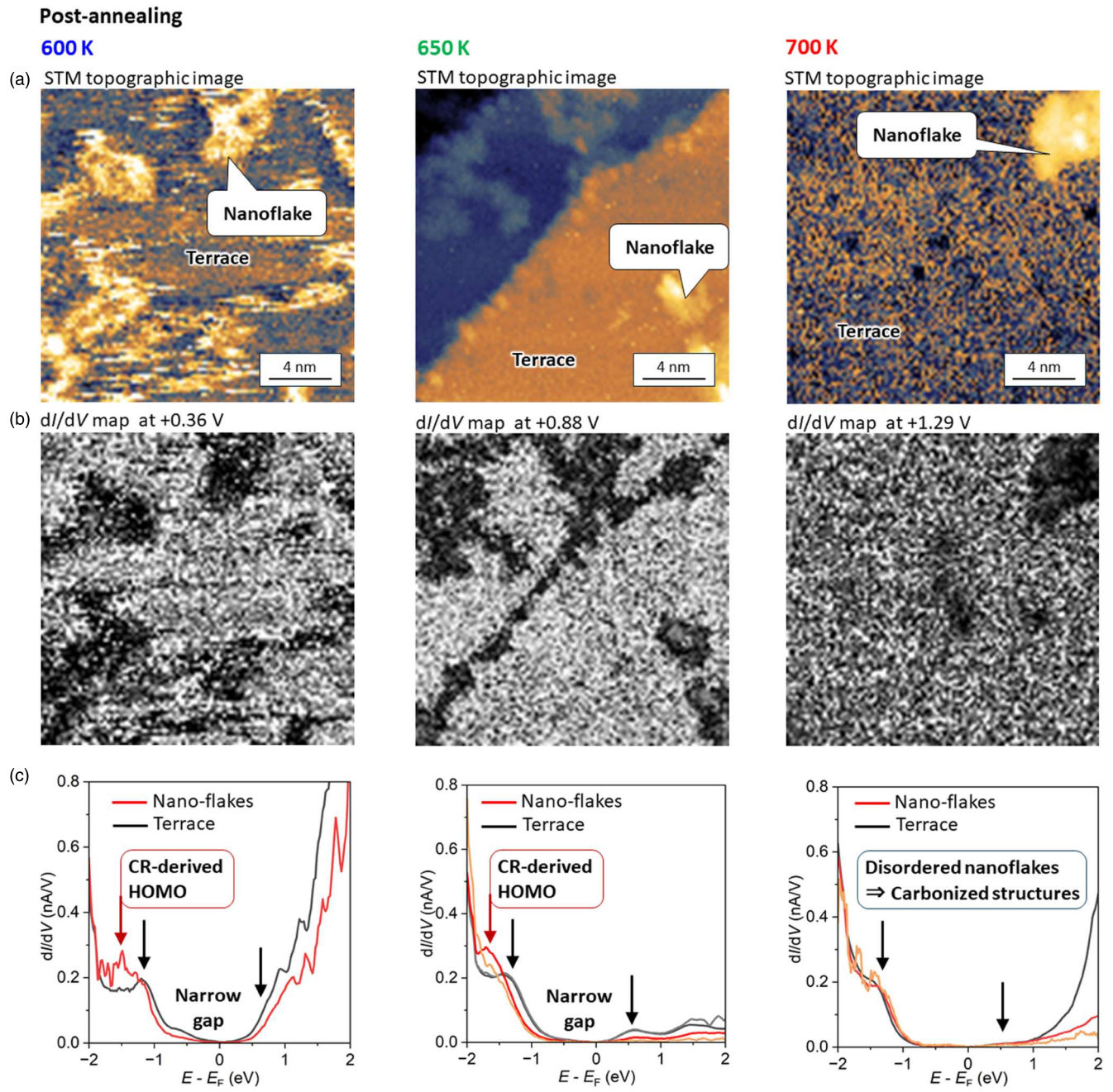

Fig. 2. Comparison of the surface electronic structures of BrCR/Cu(111) after thermal annealing at 600 K (left column), 650 K (center column), and 700 K (right column) under UHV conditions. (a) STM topographic images of 0.4 ML BrCR on Cu(111) after thermal annealing in UHV (200×200 nm^2; setpoint voltage $V_s = -2$ V; setpoint tunneling current $I_t = 100$ pA (left), 250 pA (center), and 200 pA (right)). (b) Corresponding dI/dV maps acquired simultaneously with the topographic images at left: +0.36 V (left), +0.88 V (center), and +1.29 V (right). Brighter (darker) contrast indicates a higher (lower) LDOS. (c) dI/dV spectra measured on terraces (black) and nanoflakes (red). E_F denotes the Fermi energy.

their geometric height remains similar to that of the BrCR SAM prior to annealing. However, as shown in Fig. 1(e), we observe a pronounced decrease in the apparent height after annealing. This result indicates that the CR-derived nanoflakes are positioned closer to the Cu substrate than the BrCR SAM before annealing, implying a reduced molecule–substrate distance.

4. Conclusions

In summary, we have demonstrated the evolution of intermediate states during the on-surface synthesis of 1D polymer chains from a BrCR precursor on Cu(111), investigated using a UHV STM/STS setup at 300 K. STM topographic images and STS measurements clearly show that thermal annealing above 650 K induces a drastic structural and electronic transformation: the 1D polymer chains disappear and are replaced by densely packed, CR-derived triangular-like nanoflakes. These nanoflakes exhibit metal-like LDOS features that are markedly different from those of the original semiconducting BrCR molecules. In contrast, annealing at 700 K leads to the decomposition of the CR species, as no molecular orbital features are observed in the spectra. Therefore, thermal annealing at approximately 650 K represents a critical threshold for tuning the electronic properties of the CR monolayer film on Cu(111) from semiconducting to metallic behavior.

© 2026 The Japan Society of Applied Physics. All rights, including for text and data mining, AI training, and similar technologies, are reserved.

Acknowledgments

This work was supported by JSPS KAKENHI (Grant No. 23H02033), the Murata Science Foundation, the Shorai Foundation for Science and Technology, the TEPCO Memorial Foundation, the Casio Science Promotion Foundation, and the Toshiaki Ogasawara Memorial Foundation. We thank Mr. Haruto Seki (Chiba University) for his technical support.

Conflicts of interest

The authors declare no competing financial interest.

Author contributions

T. K. Y. conceived and supervised the study and wrote the original manuscript. All co-authors critically reviewed and revised the manuscript. STM and STS measurements were performed by T. K. and T. K. Y. BrCR was synthesized by M. H.

ORCID iDs

Toyo Kazu Yamada https://orcid.org/0000-0001-5185-6472

1) T. Hosokai, M. Horie, T. Aoki, S. Nagamatsu, S. Kera, K. K. Okudaira, and N. Ueno, "Change in molecular conformation of dibenzo-crown ether induced by weak molecule−substrate interaction," J. Phys. Chem. C **112**, 4643 (2008).
2) A. Ohira, M. Sakata, C. Hirayama, and M. Kunitake, "2D-Supramolecular arrangements of Dibenzo-18-Crown-6-Ether and its inclusion complex with potassium ion by potential controlled adsorption," Org. Biomol. Chem. **1**, 251 (2003).
3) S.-C. Cheng, C.-H. Wang, Y.-C. Lin, Y. Tsuchido, Y. Suzaki, Y. Sei, T.-S. Kuo, and M. Horie, "Photoinduced mechanical motions of pseudorotaxane crystals composed of azobenzene and ferrocenyl groups on an axle and a crown ether ring," ACS Appl. Mater. Interfaces **12**, 50002 (2020).
4) F. Nishino et al., "Reversible sliding motion by hole-injection in ammonium-linked ferrocene, electronically decoupled from noble metal substrate by crown-ether template layer," Small **21**, 2408217 (2025).
5) T. K. Yamada, R. Nemoto, H. Ishii, F. Nishino, Y.-H. Chang, C.-H. Wang, P. Krüger, and M. Horie, "Designing 2D stripe winding network through crown-ether intermediate Ullmann coupling on Cu(111) surface," Nanoscale Horiz. **9**, 718.
6) R. Nemoto, P. Krüger, A. N. Putri Hartini, T. Hosokai, M. Horie, S. Kera, and T. K. Yamada, "Well-ordered monolayer growth of crown-ether ring molecules on Cu(111) in ultra-high vacuum: an STM, UPS, and DFT study," J. Phys. Chem. C **123**, 18939 (2019).
7) Y. Liang, J. Wang, R. Yin, Z. Wang, X. Wang, J. Meng, S. Tan, C. Ma, Q. Li, and B. Wang, "Pyrolysis conversion of crown-ether-based covalent networks to kagome metal-organic frameworks on Au(111) and Ag(111)," Carbon Trends **19**, 100474 (2025).
8) C.-H. Wang, Y.-C. Lin, S. Bhunia, Y. Feng, P. Kundu, C. L. Stern, P.-L. Chen, J. F. Stoddart, and M. Horie, "Photosalience and thermal phase transitions of azobenzene- and crown ether-based complexes in polymorphic crystals," J. Am. Chem. Soc. **145**, 21378 (2023).
9) C.-H. Wang and M. Horie, "Photo and thermal responsive pseudorotaxane crystals comprising ferrocene-containing ammonium salts and crown ethers," Mater. Today Chem. **24**, 100852 (2022).
10) C.-H. Wang, K.-J. Chen, T.-H. Wu, H.-K. Chang, Y. Tsuchido, Y. Sei, P.-L. Chen, and M. Horie, "Ring rotation of ferrocene in interlocked molecules in single crystals," Chem. Sci. **12**, 3871 (2021).
11) R. F. Dou, D. Y. Zhong, W. C. Wang, K. Wedeking, G. Erker, L. Chi, and H. Fuchs, "Structures and stability of ferrocene derivative monolayers on Ag(110): scanning tunneling microscopy study," J. Phys. Chem. C **111**, 12139 (2007).
12) M. Ormaza, P. Abufager, N. Bachellier, R. Robles, M. Verot, T. Le Bahers, M.-L. Bocquet, N. Lorente, and L. Limot, "Assembly of ferrocene molecules on metal surfaces revisited," J. Phys. Chem. Lett. **6**, 395 (2015).
13) T. K. Yamada, S. Kanazawa, K. Fukutani, and S. Kera, "Growth of transition-metal cobalt nanoclusters on 2D covalent organic frameworks," J. Phys. Chem. C **128**, 1477 (2024).
14) T. K. Yamada, T. Abe, N. M. K. Nazriq, and T. Irisawa, "Electron-bombarded ⟨110⟩-oriented tungsten tips for stable tunneling electron emission," Rev. Sci. Instrum. **87**, 033703 (2016).
15) T. Yamaguchi, E. Inami, Y. Goto, Y. Sakai, S. Sasaki, T. Ohno, and T. K. Yamada, "Fabrication of tungsten tip probes within 3 s by using flame etching," Rev. Sci. Instrum. **90**, 063701 (2019).
16) Y. Goto, R. Suizu, Y. Noguchi, and T. K. Yamada, "Oxidative vaporization etching for molybdenum tip formation in air," Appl. Surf. Sci. **542**, 148642 (2021).
17) Y. Yamagishi, S. Nakashima, K. Oiso, and T. K. Yamada, "Recovery of nanomolecular electronic states from tunneling spectroscopy: LDOS of low-dimensional phthalocyanine molecular structures on Cu(111)," Nanotechnology **24**, 395704 (2013).
18) V. A. Ukraintsev, "Data evaluation technique for electron-tunneling spectroscopy," Phys. Rev. B **53**, 11176 (1996).
19) I. Horcas, R. Fernández, J. M. Gómez-Rodríguez, J. Colchero, J. Gómez-Herrero, and A. M. Baro, "WSXM : a software for scanning probe microscopy and a tool for nanotechnology," Rev. Sci. Instrum. **78**, 013705 (2007).
20) M. A. Barral, M. Weissmann, and A. M. Llois, "Characterization of the surface states of Co(0001), Co(111), and ultrathin films of Co on Cu(111)," Phys. Rev. B **72**, 125433 (2005).
21) E. Inami, M. Yamaguchi, T. Yamaguchi, M. Shimasaki, and T. K. Yamada, "Controlled deposition number of organic molecules using quartz crystal microbalance evaluated by scanning tunneling microscopy single-molecule-counting," Anal. Chem. **90**, 8954 (2018).
22) R. Courths, H. Wern, and S. Hüfner, "The tamm surface state on Cu(111) and Ag(111)," Solid State Commun. **61**, 257 (1987).
23) G. Hörmandinger, "Imaging of the Cu(111) surface state in scanning tunneling microscopy," Phys. Rev. B **49**, 13897 (1994).
24) P. Ruffieux et al., "On-surface synthesis of graphene nanoribbons with zigzag edge topology," Nature **531**, 489 (2016).

© 2026 The Japan Society of Applied Physics. All rights, including for text and data mining, AI training, and similar technologies, are reserved.